

Recombination Mechanisms in Solar Silicon Materials

A.R. Peaker, V.P. Markevich, B. Hamilton, M. Halsall

peaker@manchester.ac.uk

www.manchester.ac.uk/research/a.peakier/

*Photon Science Institute
University of Manchester,
Manchester, M13 9PL, UK*



Outline

- **Solar silicon**
- **Recombination & techniques**
- **Czochralski Si and continuous Cz**
- **Cast Si & nano-precipitates**
- **Kerfless Si**
- **Hydrogen passivation (Pt, Ti, Fe)**

Silicon materials

Electronic grade Fz and Cz are regarded as expensive for solar
 $\text{SiO} + \text{C} > \text{Si} > \text{HSiCl}_3 > \text{poly Si} > \text{single crystal Cz or FZ growth}$

Cost reductions in materials achieved by lower cost polycrystalline feed stock, cheaper growth methods, reducing or eliminating cutting losses.

In general the result of these approaches is a reduction in cell efficiency because of decreased minority carrier lifetime.

Much effort by many groups devoted to improving lower cost Si ... novel growth approaches, gettering, passivation etc

BUT material cost reductions can result in an increase in cost per kWh at the system level due to reductions in efficiency.



Silicon material growth technologies

Cz and Fz Si grown from Siemens process poly are very pure, no compensation, TM metals usually undetectable (due to high segregation coefficient from melt $\sim 10^{-5}$), $< 10^{16}$ carbon, oxygen at 10^{17} to 10^{18} cm^{-3} in Cz, Very few extended defects.

Cast Si contains contamination from crucible (edges and base contaminated by diffusion), TM impurities in melt are segregated to last grown region (usually top) Seeding can produce large monocrystalline areas but many extended defects are present.

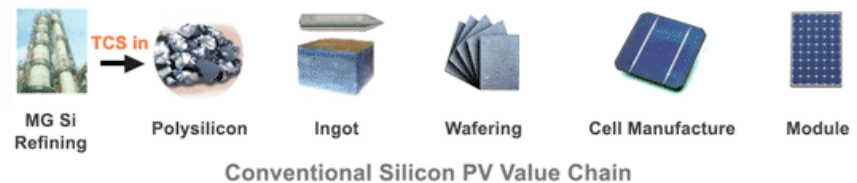


Continuous Cz grows ingots from a replenished melt. TM concentration expected to increase as growth progresses.

photo from Confluence



Kerfless is a generic term for silicon which does not need conventional slicing. In this talk I deal only with epi on porous Si such as the Canon ELTRAN process.



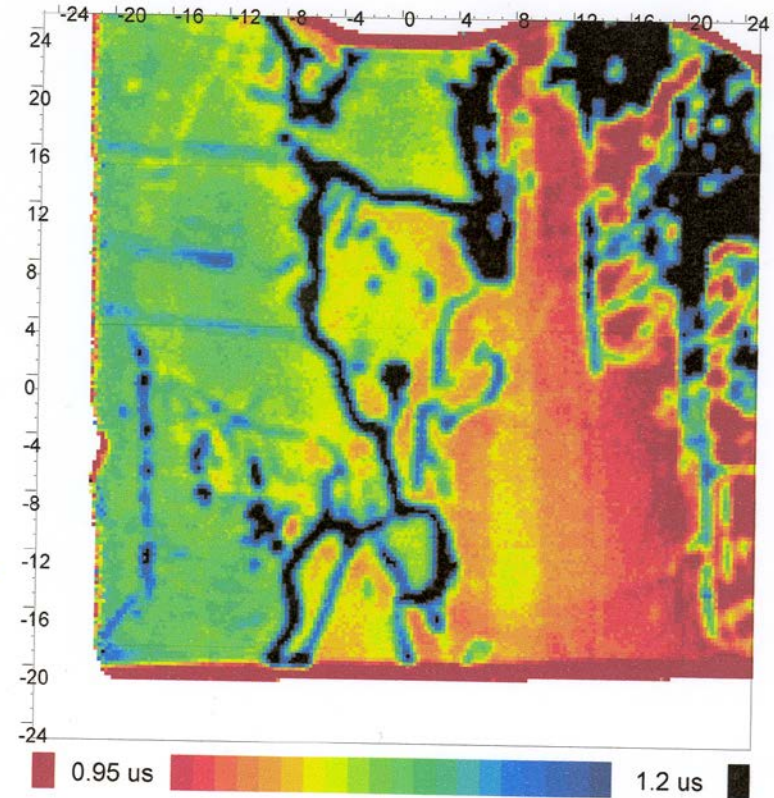
Objectives

The aim of our work is to find the dominant recombination paths degrading efficiency in various types of crystalline solar silicon and to trace the defect origins.

Principal techniques that we are using are lifetime measurements, variants of DLTS and modelling defect and defect reactions.

We work mostly on material prior to processing and use annealing and gettering to simulate process steps in a way we can control but sometimes we use part process slices and cells.

There are some very difficult issues in cast silicon because of the wide range of defects and large variations in lifetime across a slice.

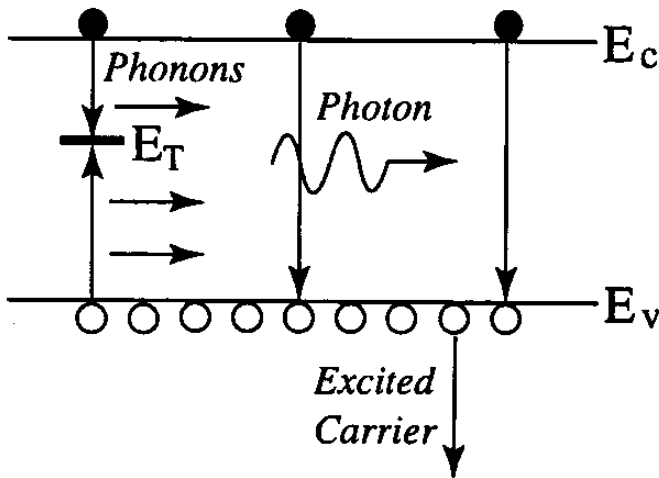


Lifetime map using Semilab WT2000 of a 4cm square section of a slice from near the top of a cast ingot grown from upgraded metallurgical Si. The low lifetime ($\sim 1\mu\text{s}$) is due to clusters of dislocations decorated with TMs

Recombination Processes

In general four key processes need to be considered:

- **Shockley-Read-Hall (depends on defect concentration)**
- **Surface (depends on surface states and thickness)**
- **Radiative (crucial in direct band gap materials)**
- **Auger (important in highly doped material)**



Because recombination rates are additive, any of these mechanisms can dominate the carrier lifetime ie:

$$\tau_r = \frac{1}{\tau_{\text{SRH}}^{-1} + \tau_{\text{rad}}^{-1} + \tau_{\text{Auger}}^{-1}}$$

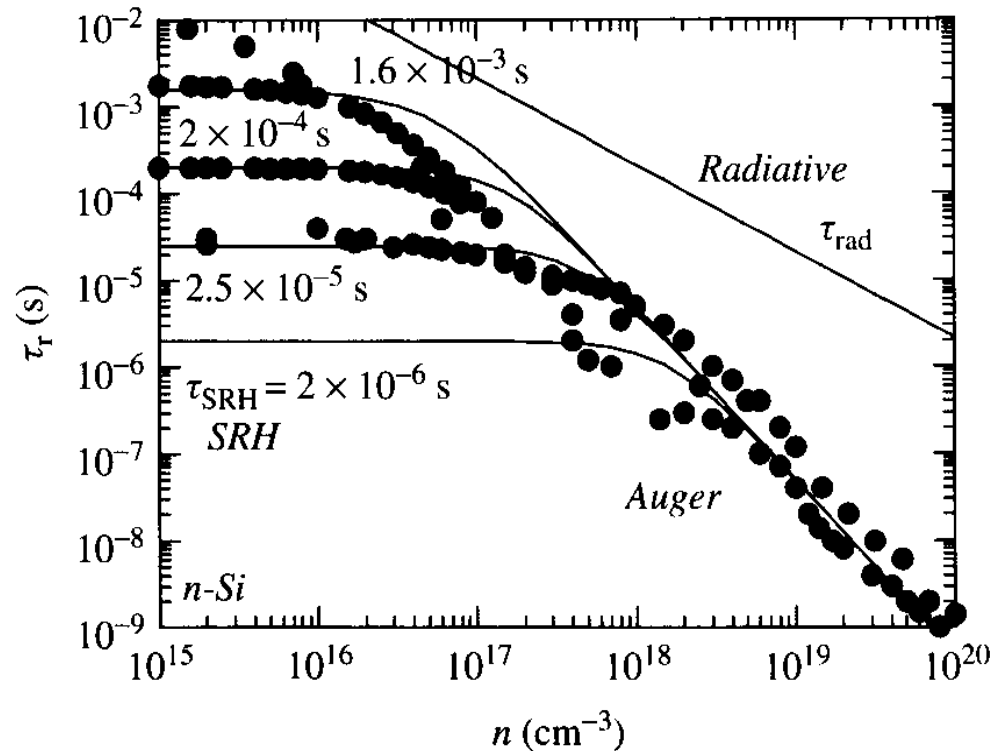
Recombination

Radiative recombination is insignificant so the bulk lifetime depends on SRH and Auger

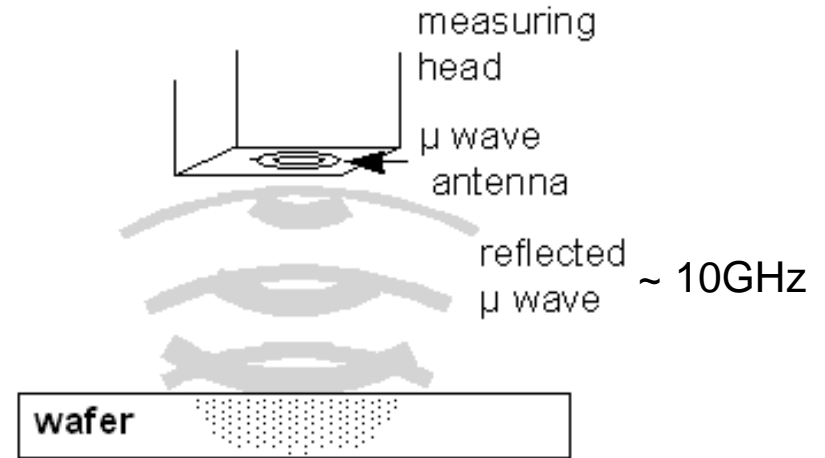
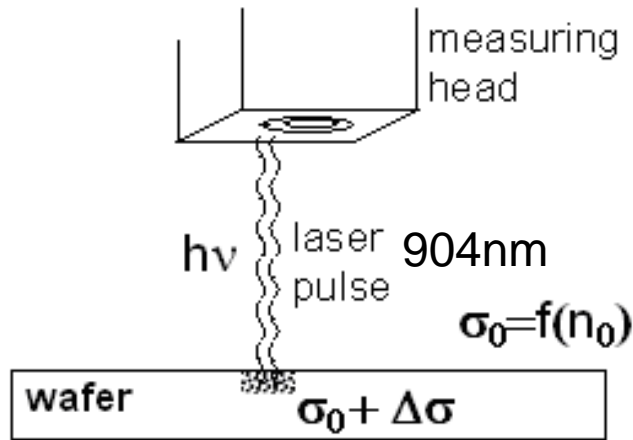
$$\tau_{\text{Auger}} \approx \frac{1}{C_p(p_0^2 + 2p_0\Delta n + \Delta^2 n)}$$

$$C_p \approx 10^{-31} \text{ cm}^6/\text{s}, \quad C_n \approx 2.8 \times 10^{-31}$$

Band to band Auger recombination rate increases as the square of carrier concentration. It dominates at high carrier concentrations and/or very high excitation densities.



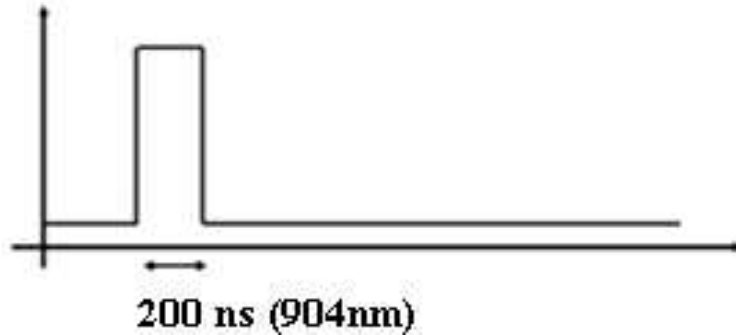
SRH recombination depends on defect concentration and defect properties



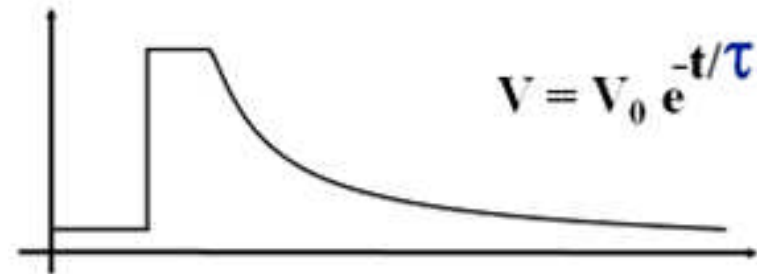
σ : conductivity
 n : free carrier concentration

measurable lifetime range 10ns to 30ms at quite high excitation density ($10^{14} - 10^{16}$ excess carriers cm^{-3} in $100\mu\text{s}$ material)

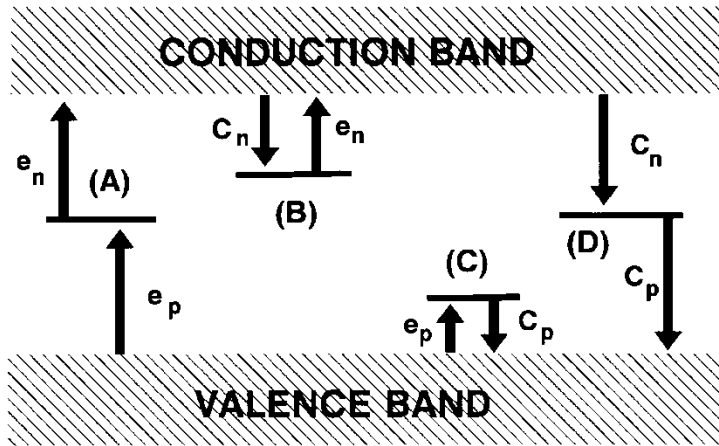
Excitation pulse



Detected μw signal



Shockley-Read-Hall recombination



Process D

For the case of low excitation density ($\Delta p \ll n_o$ in n type and $\Delta n \ll p_o$ in p type) the recombination lifetime is given for n type and p type respectively by:

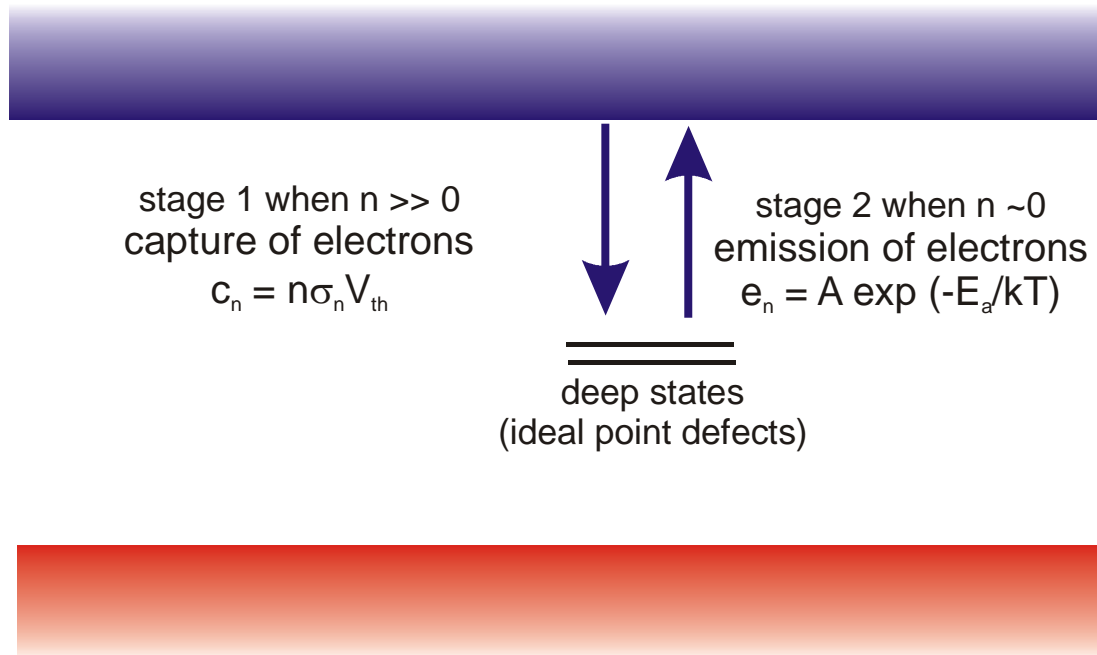
$$\tau_p = \frac{1}{\sigma_p v_{th} N_T}; \quad \tau_n = \frac{1}{\sigma_n v_{th} N_T}$$

Where v_{th} is the thermal velocity, N_T the defect concentration and σ the minority carrier capture cross section.

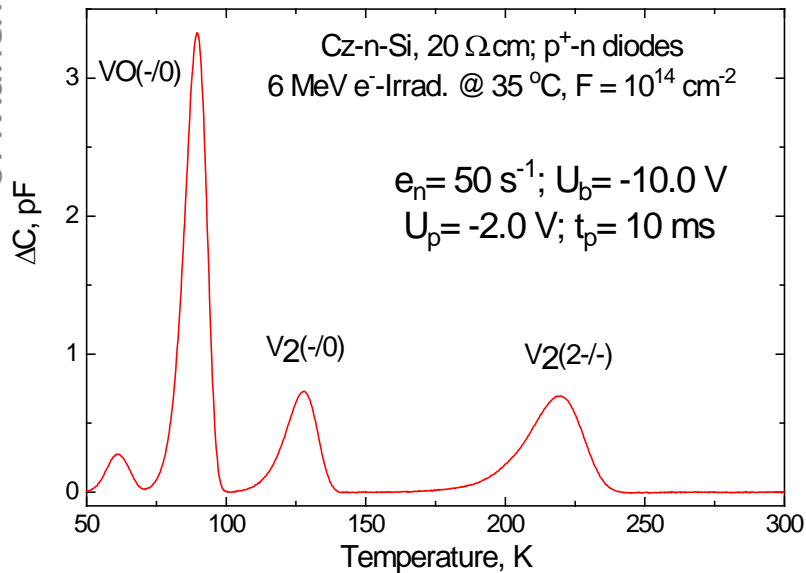
For the case of higher injection level the majority carrier capture rate may start to limit the overall recombination rate and the minority carrier lifetime will increase ie the SRH process will start to saturate.

Measuring defect parameters

In order to quantify SRH recombination we need to measure the defect energy position in the gap, the concentration and the capture cross sections. Deep Level Transient Spectroscopy (DLTS) and its variants enable us to do this. The measurements use a two stage carrier capture and emission process (trapping). To do this we normally measure the charge exchange in a depletion region of a p-n junction or Schottky barrier by monitoring the capacitance.

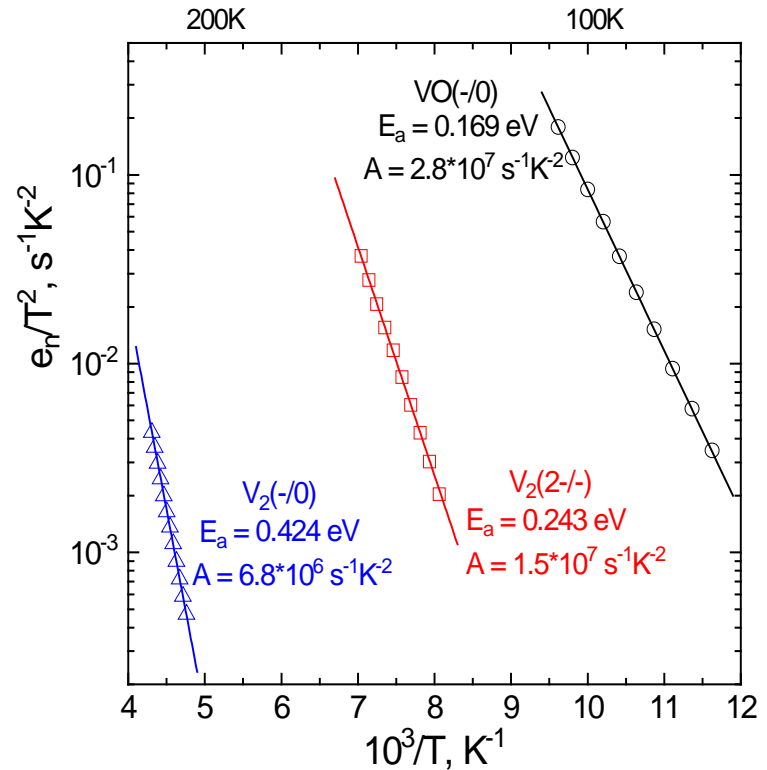


DLTS scan: irradiated n-type silicon



ΔC (the vertical axis) is $C(t_1) - C(t_2)$ where t_1, t_2 are times from the start of the carrier emission transient

By repeating the temperature scan with different settings of t_1 and t_2 the system filters out different rates (rate windows) and so each T_{max} corresponds to the temperature at which the trap emits carriers at that rate window.



These Arrhenius plots provide a fingerprint of the defects which gives important clues as to the chemical identity

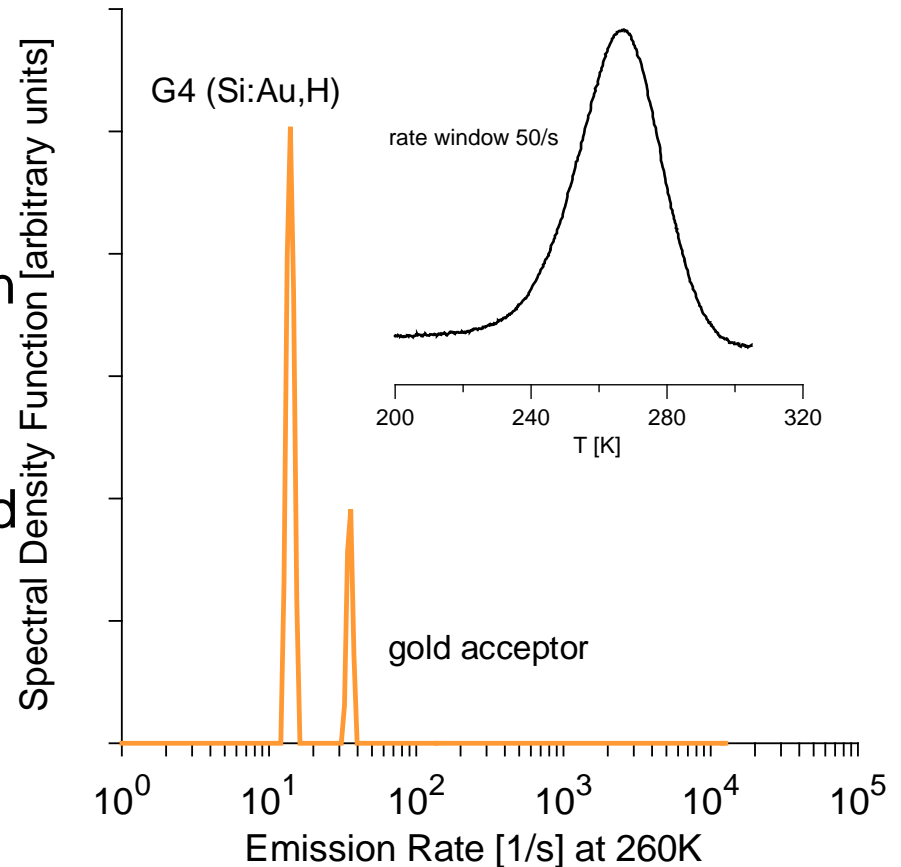
DLTS is absolutely quantitative giving us concentration and data from which we can derive many defect parameters with very good detectivity. But the energy resolution of DLTS is poor; limited by instrumental broadening to $(e_1/e_2) \geq 15 \dots$ so states separated by $<50\text{meV}$ appear as one DLTS peak.

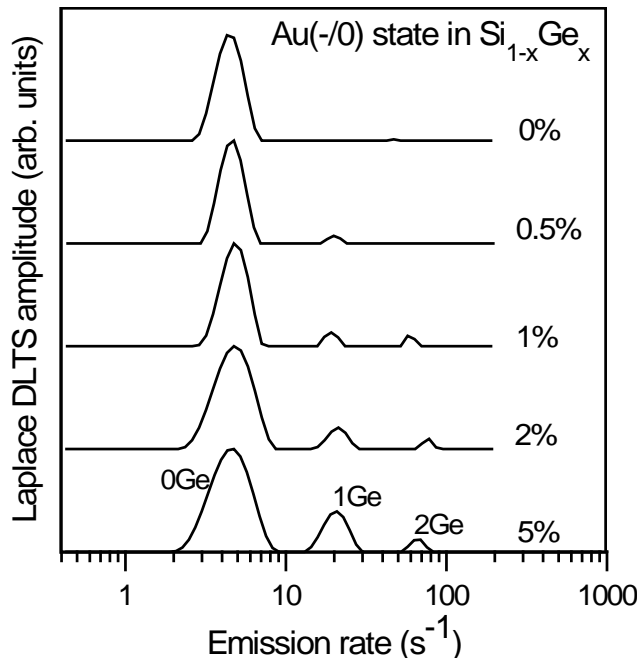
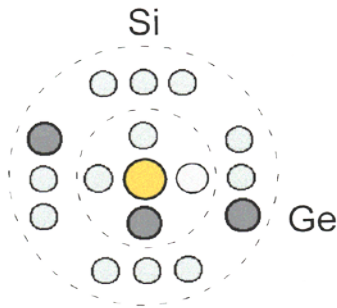
DLTS confuses similar states and throws away much of the physical information which is very important in understanding defects.

So we developed Laplace DLTS (resolution 2meV) which is compared with conventional DLTS in the diagram for Si:Au and Si:Au,H

J. Appl. Phys, **76**, 194, (1994)

J. Appl. Phys, Review, **96**, 4689, (2004)

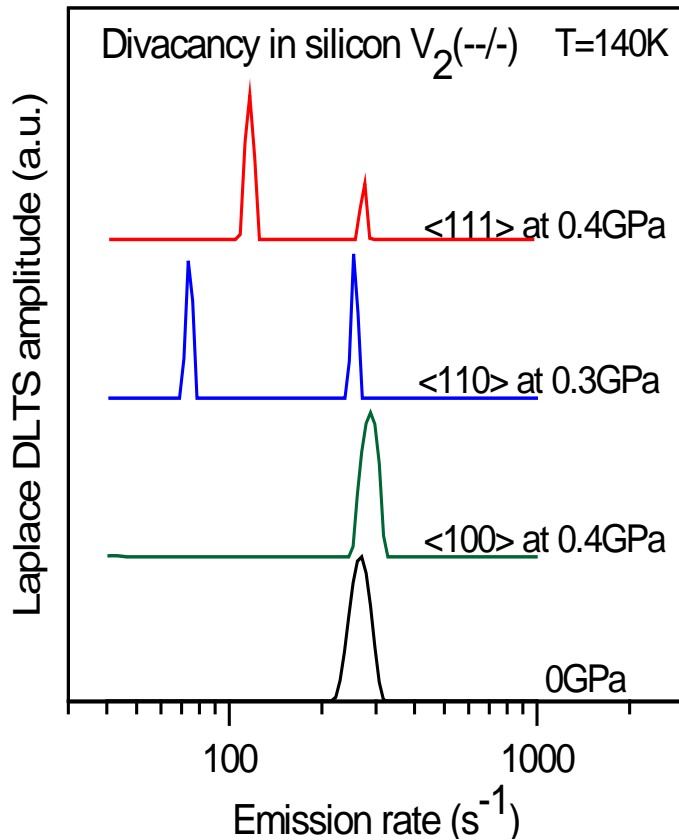




Example SiGe:Au

- Au in has 4 nearest neighbours and 12 second nearest neighbours which can be Si or Ge
- The electron binding energy to the gold is modified by the local environment (ie Si or Ge)
- LDLTS can be used to quantify the local environment and so determine site preferences

example: double acceptor state of the silicon di-vacancy



- applying stress in the three major directions reveals the apparent symmetry of this diamagnetic state in a region $<1\mu m$ thick
- comparison of the derived values of piezo-spectroscopic tensor components with those obtained from theoretical calculations helps to decide if this is the true symmetry and possibly reveals the defect structure. We conclude V_2^{2-} has static trigonal symmetry with no measurable Jahn Teller effect (unlike V_2^-)

	splitting ratios		
system	<111>	<110>	<100>
trigonal (D_{3d})	3:1	3:3	3:0

So how have we applied these techniques to pick out the dominant recombination paths in specific materials?

I will deal with different materials separately:

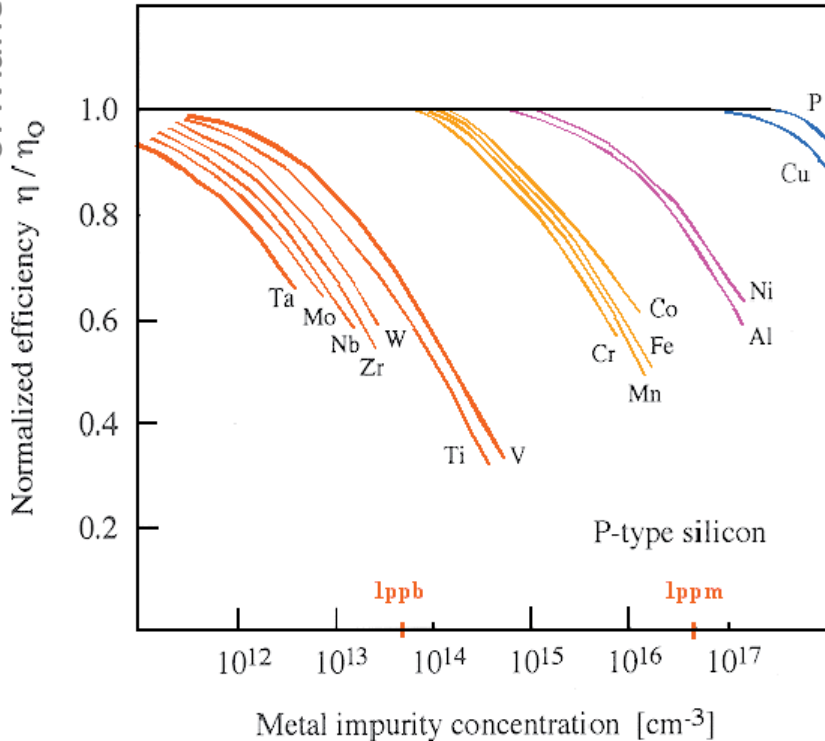
- **Czochralski Si and continuous Cz**
- **Cast Si & nano-precipitates**
- **Kerfless Si**

Then present work we have done on:

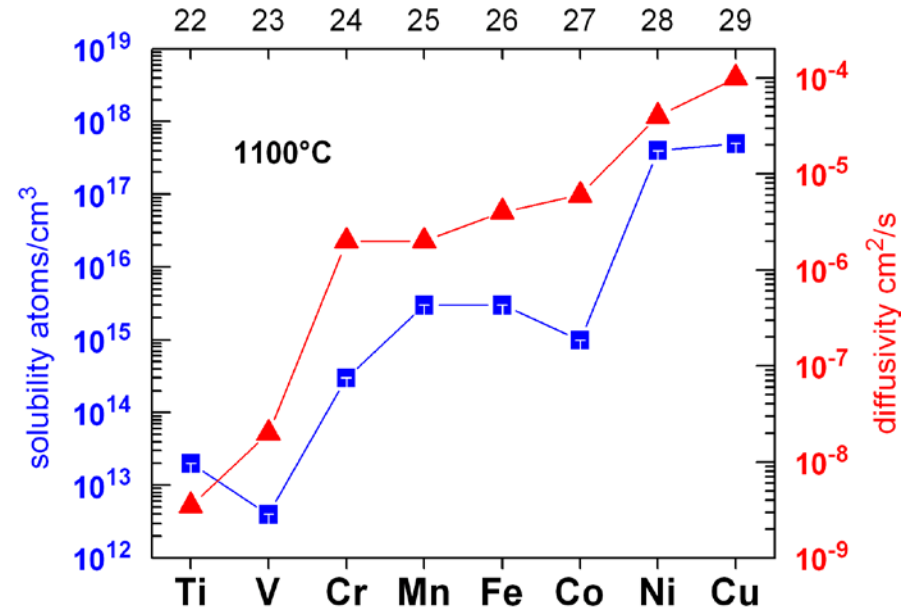
- **Hydrogen passivation (Au, Ti, Fe)**

but first a reminder of some properties of TMs

Westinghouse experiment on single crystal Cz silicon intentionally contaminated with metals

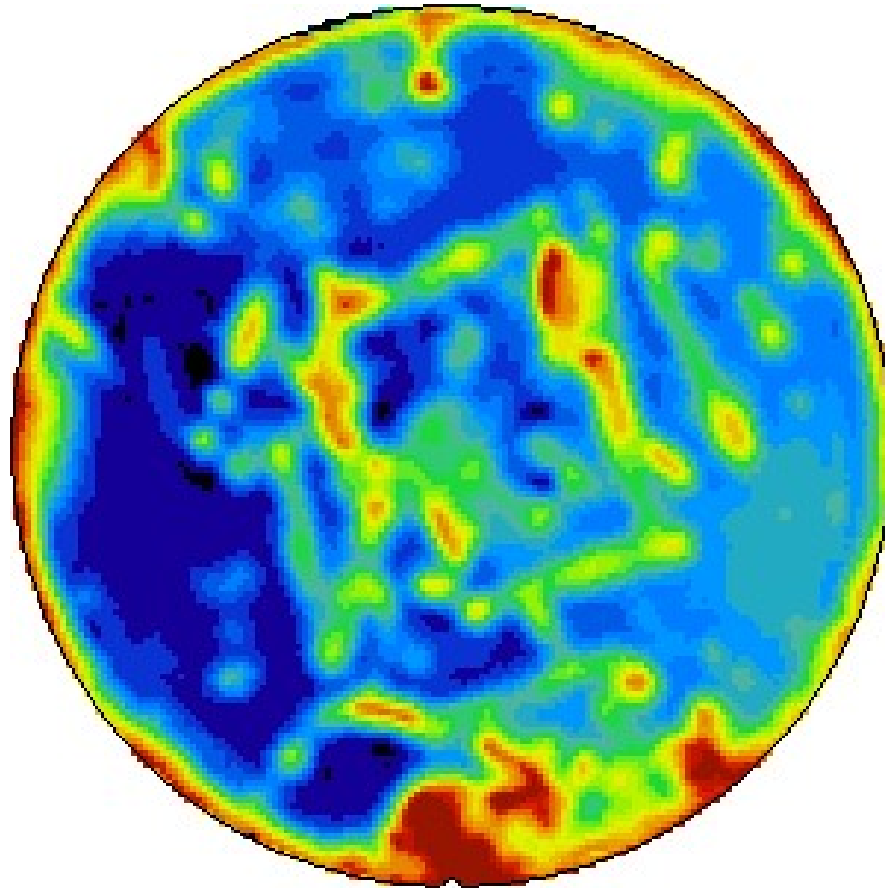


Mg 12	3d transition metals										Al 13
Ca 20	Sc 21	Ti 22	V 23	Cr 24	Mn 25	Fe 26	Co 27	Ni 28	Cu 29	Zn 30	Ga 31
Sr 38	Y 39	Zr 40	Nb 41	Mo 42	Tc 43	Ru 44	Rh 45	Pd 46	Ag 47	Cd 48	In 49



The higher atomic number 3d transition metals have higher diffusivities so are more easily gettered.

Electronic grade conventional Cz Si ... contamination after dielectric deposition

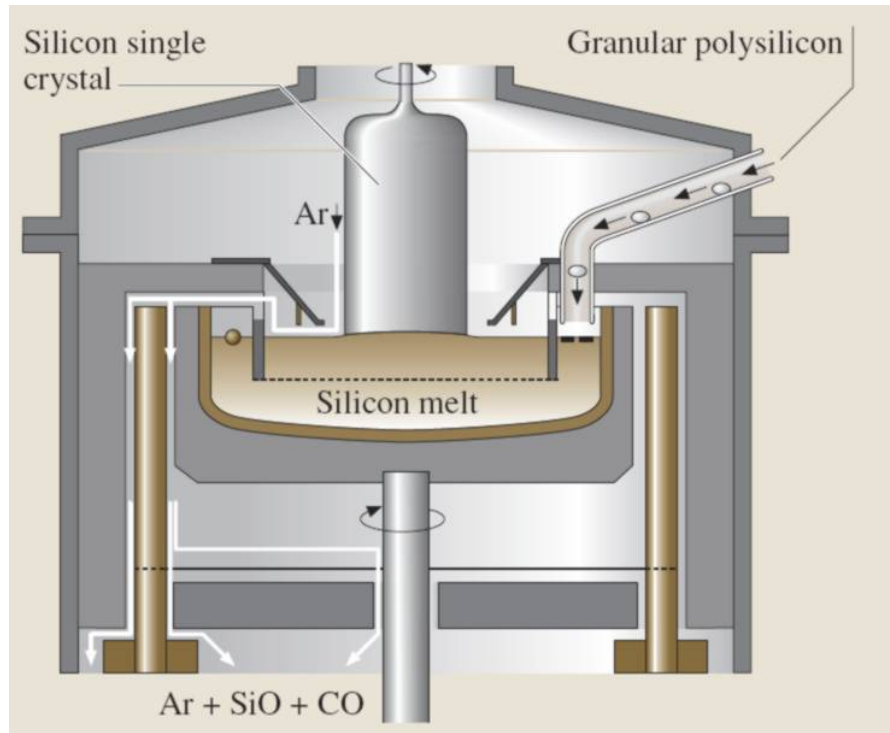


8 inch electronic grade p-type 20 Ω -cm ($p=6 \times 10^{14} \text{ cm}^{-3}$) Si slice after deposition of silicon nitride on both sides. Bad handling has resulted in localised contamination.

What can we detect in DLTS?
Commercial systems can usually see 10^{-4} of the carrier concentration. Specialist systems between 10^{-5} and 2×10^{-6} .

So a commercial system could quantify and identify the contamination in the red regions (1ms, $\sim 10^{11} \text{ Fe}_i \text{ cm}^{-3}$) but not at this Fe_i level in 1 Ω -cm p-type ($p=10^{16} \text{ cm}^{-3}$)

“Continuous” Czochralski (CCz)



Polysilicon and dopant are fed into a section of the melt separated from the ingot as growth progresses

Ingots are re-seeded without cooling the melt.

As TMs have a very low segregation coefficient it would be expected that they would accumulate in the melt decreasing the carrier lifetime.

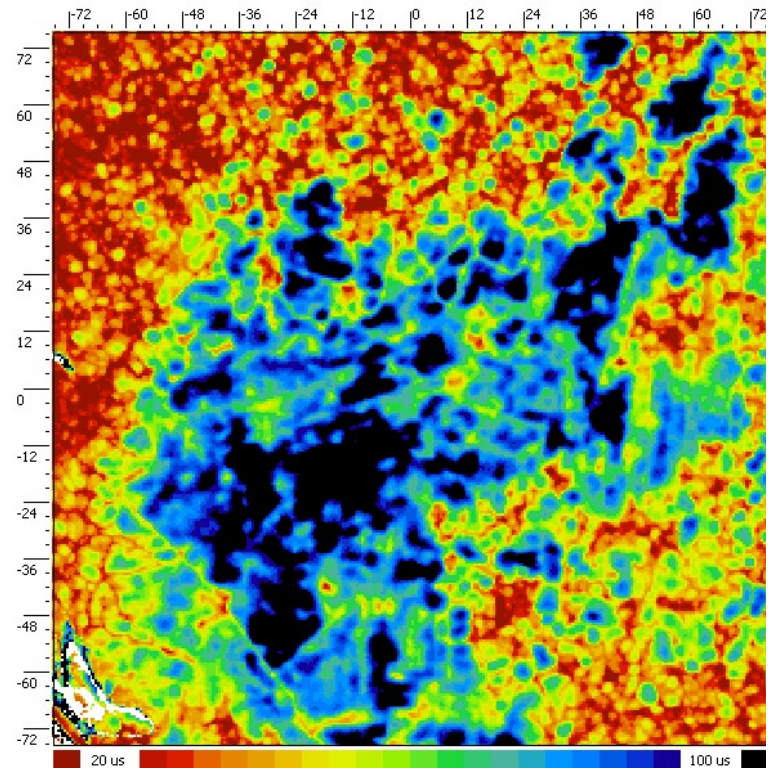
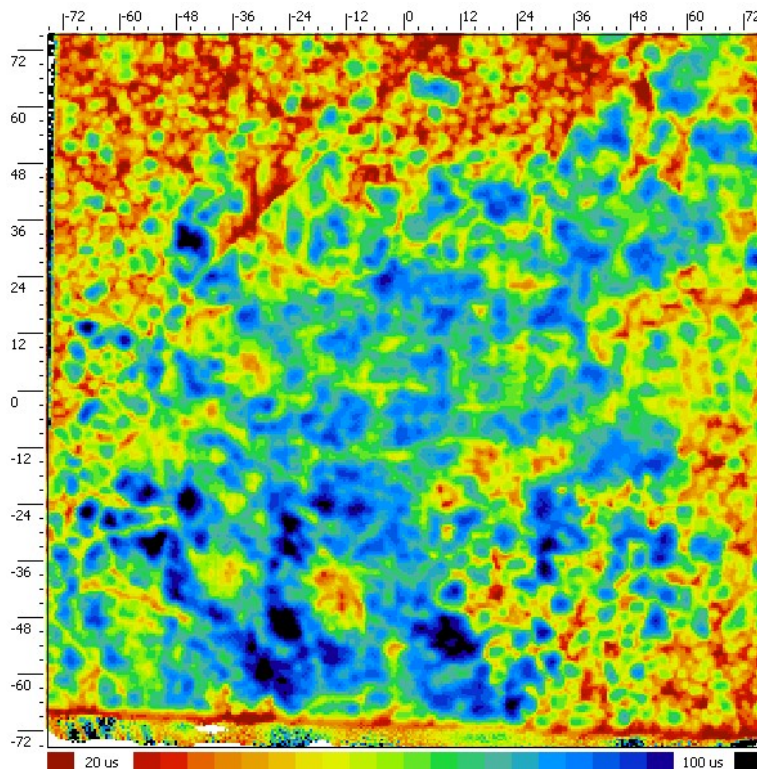
However on the ingots we have measured (grown from fluidised bed feedstock) it is not the TMs which limit the number of ingots which can be grown ... ms lifetimes are maintained

CCz was originally developed for electronic grade material in the 90s but recently was seen as a cheaper route to Cz solar material by Confluence then GT. Several companies are now evaluating the method

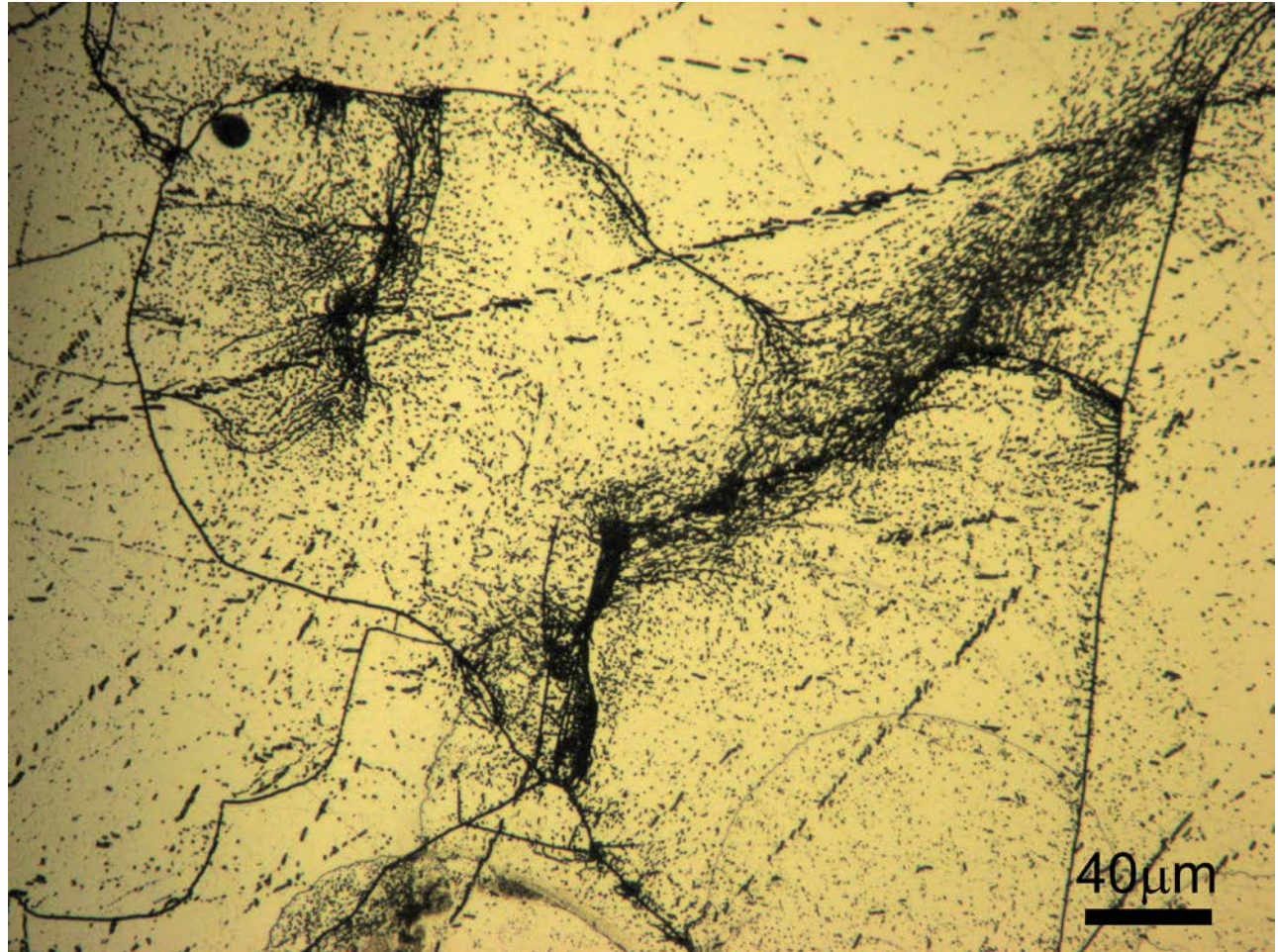
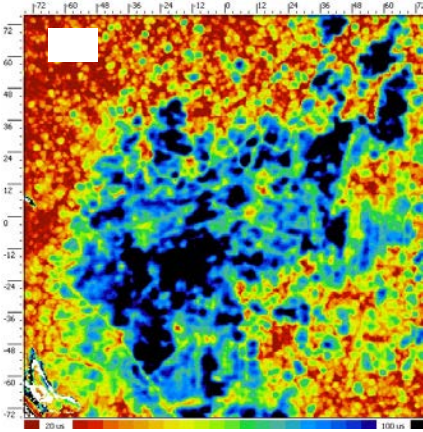
p-type mono-cast wafers lifetime map from WT2000 ~0.5mm resolution
150mm square sample lifetime range 20 μ s (red) -100 μ s (blue)

as received

after POCl₃ diffusion gettering

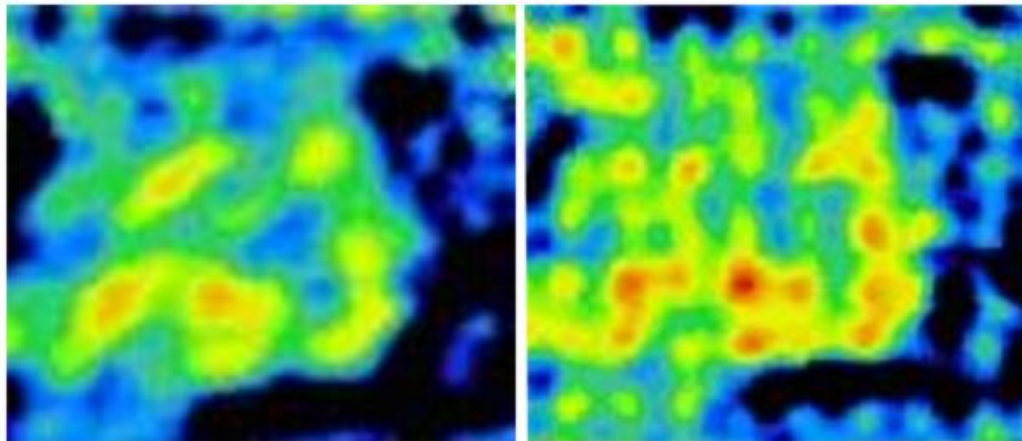
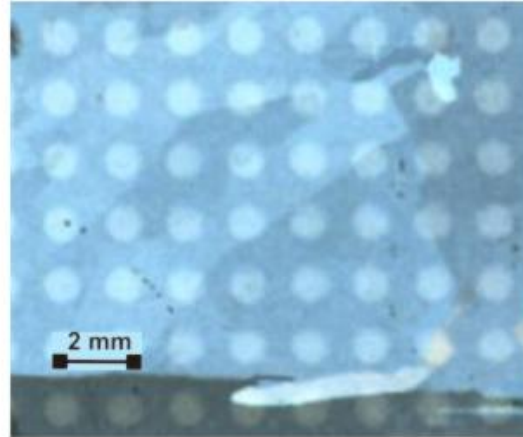


p-type mono-cast solar silicon
Secco etched optical micrograph

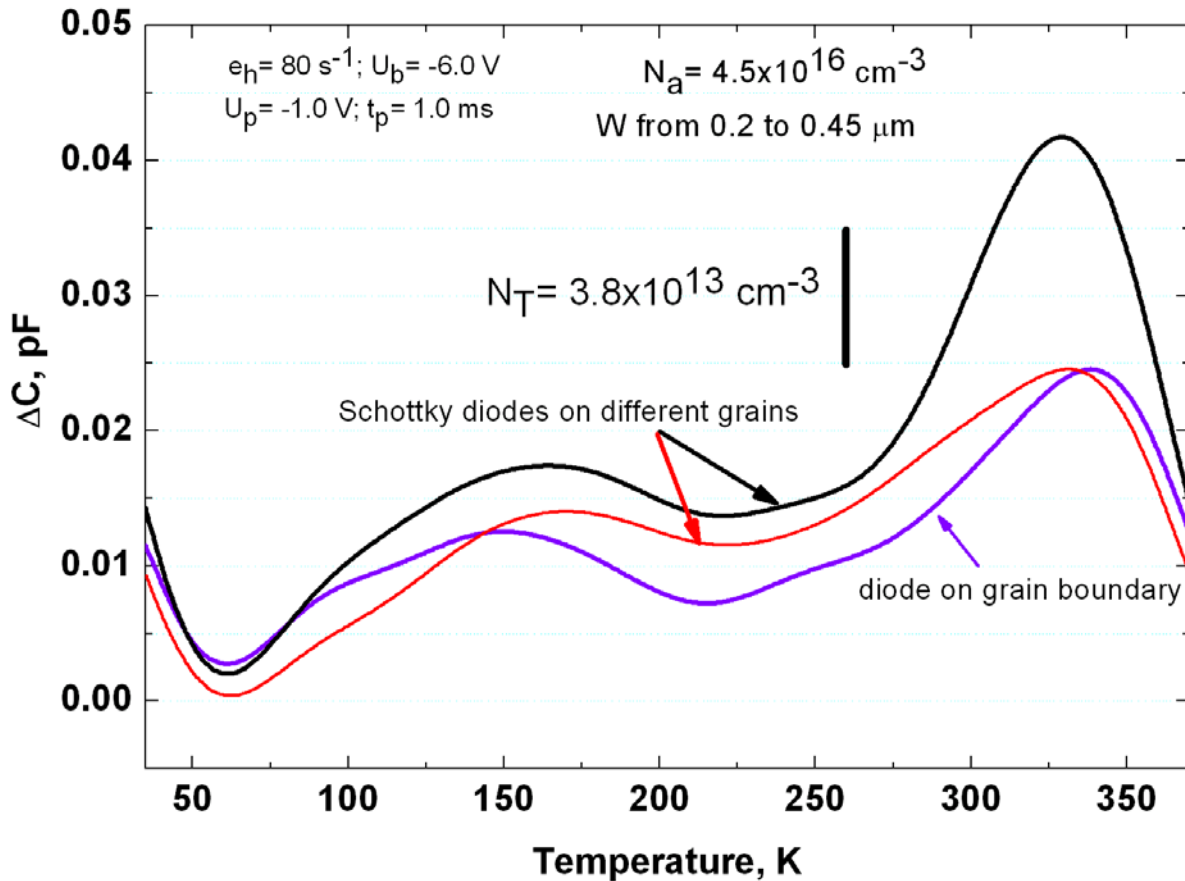


small region of a
monocast wafer
showing a wide
range of defects

Optical image and lifetime maps showing location of semi-transparent Schottky diodes



0.8 μ s  1.3 μ s



The peak around 330K shows log filling with majority carriers typical of a dislocation. The peaks in the 100 to 180K region exhibit very fast capture.

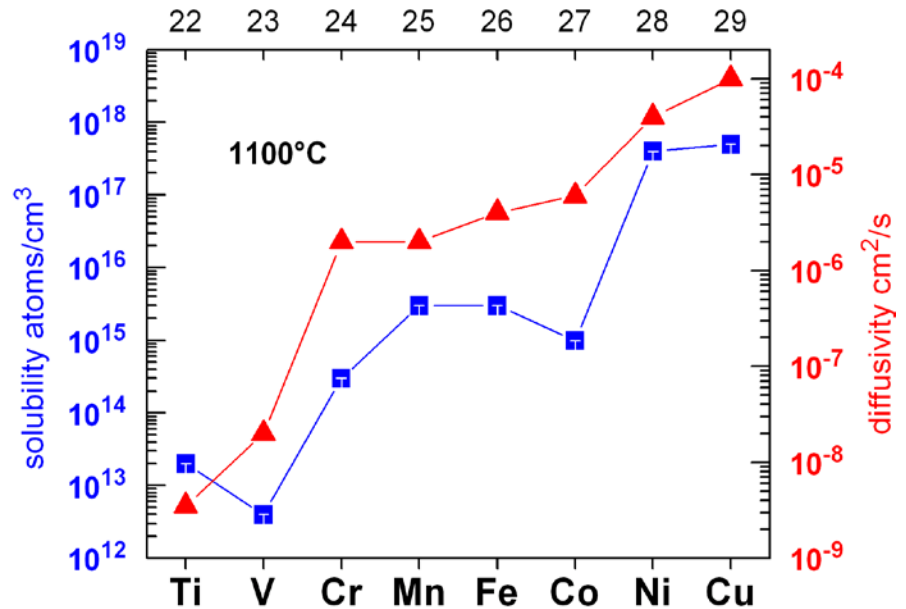
Hydrogenation reduces the 330K peak dramatically. the lower temperature peaks are less affected

Precipitated TMs in Silicon

The higher atomic number 3d transition metals have higher diffusivities. This high diffusivity with their large change of solubility with temperature creates a tendency to precipitate.

Such precipitates although detrimental to solar cells (shorts and leakage) have only a small effect on recombination.

However, we find the lower diffusivity 3d and 4d metals can form very small precipitates (nano-precipitates) which seem to be very powerful recombination centers.



Mg 12	3d transition metals										Al 13
Ca 20	Sc 21	Ti 22	V 23	Cr 24	Mn 25	Fe 26	Co 27	Ni 28	Cu 29	Zn 30	Ga 31
Sr 38	Y 39	Zr 40	Nb 41	Mo 42	Tc 43	Ru 44	Rh 45	Pd 46	Ag 47	Cd 48	In 49

Small precipitates

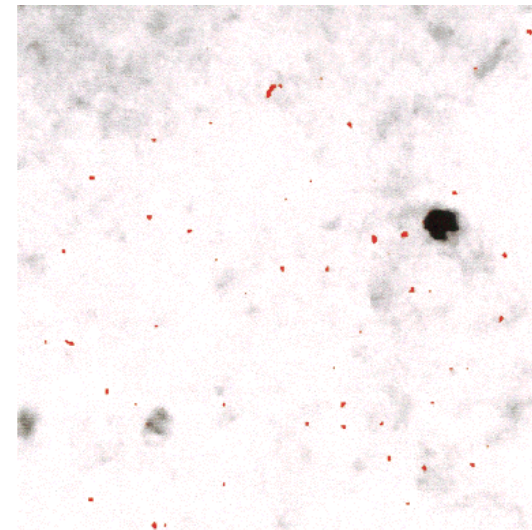
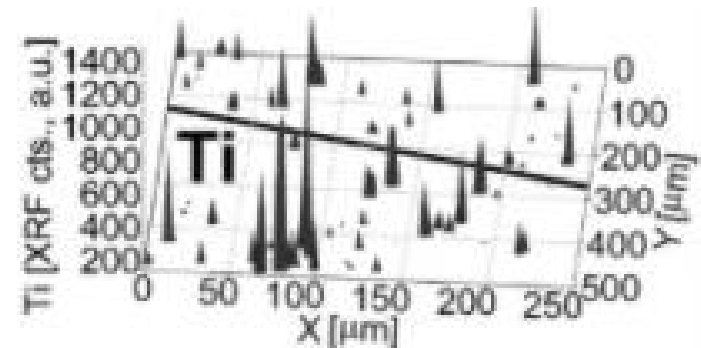
Small precipitates of slow diffusing metals have been observed previously

1) *Tonio Buonassisi et al Progress in PV Res. Appl 14, 513 (2006)*

Synchrotron-based analytical x-ray microprobe techniques of ingot-grown mc-Si using showed Ti as precipitates or oxide inclusions

2) *Maria Polignano et al. : Materials Science and Engineering B53, 300 (1998)*

TEM Energy loss images of implanted Mo in Si annealed at 1175°C for 160 min. The red dots show Mo rich regions



50 nm

Nano-precipitates

We have chosen molybdenum (a slow diffuser with low solubility) to study nano-precipitates. As a point defect at an interstitial site it is a well known as an important recombination center.

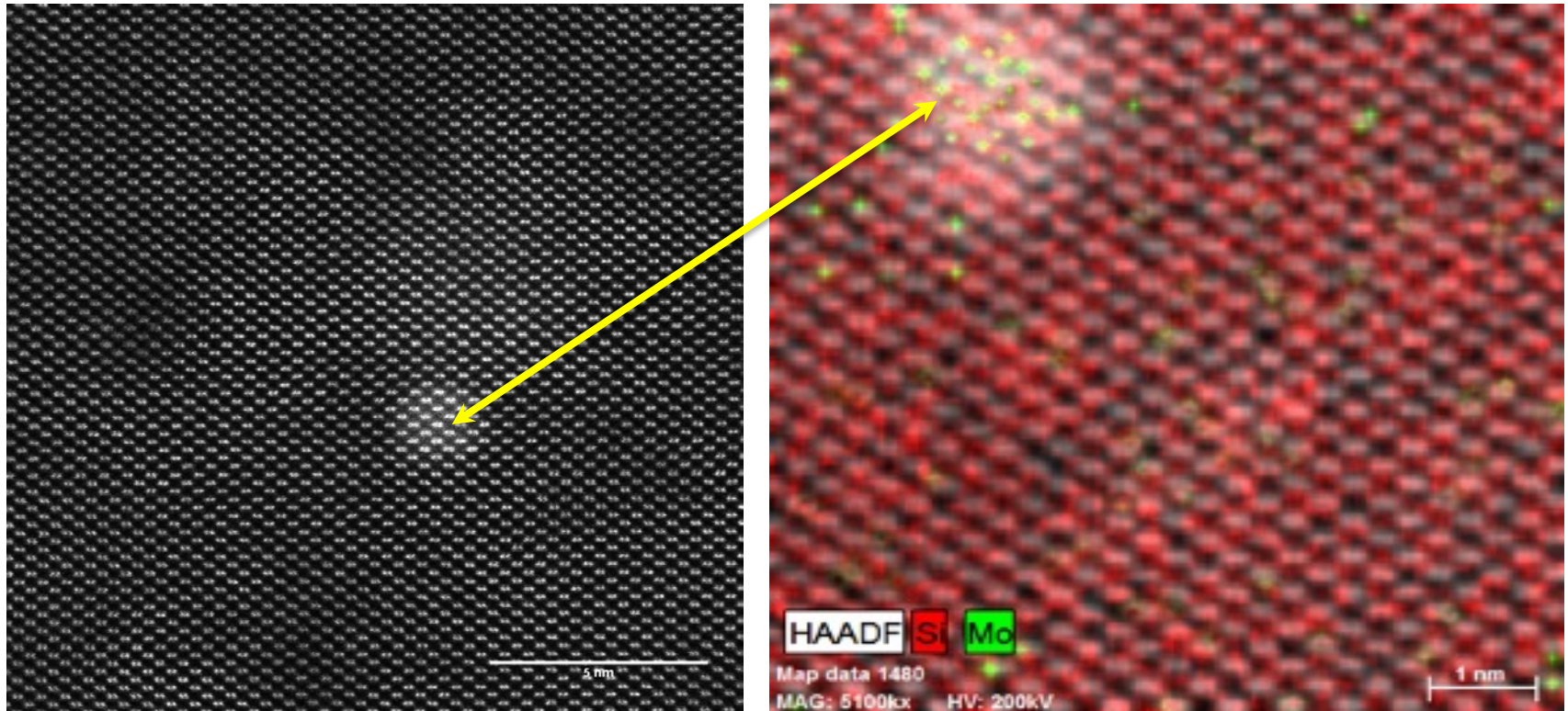
Molybdenum is present in cast solar silicon at $\sim 10^{13}$ cm³ (lower in the bottom of the ingot and higher in the top).

It is common in electronic grade Si as a contaminant of epi and in implants due to mass/charge aliasing between $^{98}\text{Mo}^{2+}$ and $(^{11}\text{B}^{19}\text{F}_2)^+$. We have studied three types of material:

- 1) **Epitaxial silicon** with Mo grown in at a concentration of $\sim 10^{13}$ cm⁻³ (measured by DLTS but below our detection limit in SIMS)
- 2) **Cz & Fz Si implanted with Mo⁺** ions at an energy of 2MeV and a dose of 5×10^{12} cm⁻² giving a peak concentration of 1.9×10^{16} cm⁻³ (SIMS) anneals between 650°C and 900°C.
- 3) Slices of **cast Si** from various ingot positions

TEM (Titan) Images

Lattice Images of Mo nano-precipitates



Scale marker at left 5nm on right 1nm

Z contrast image on left shows a region of higher density atoms. Energy Dispersive X-ray detects chemical species showing Mo atoms as green dots silicon as red. Precipitates are $\sim 2\text{nm}$ across. Image taken $\sim 0.8\mu\text{m}$ from surface.

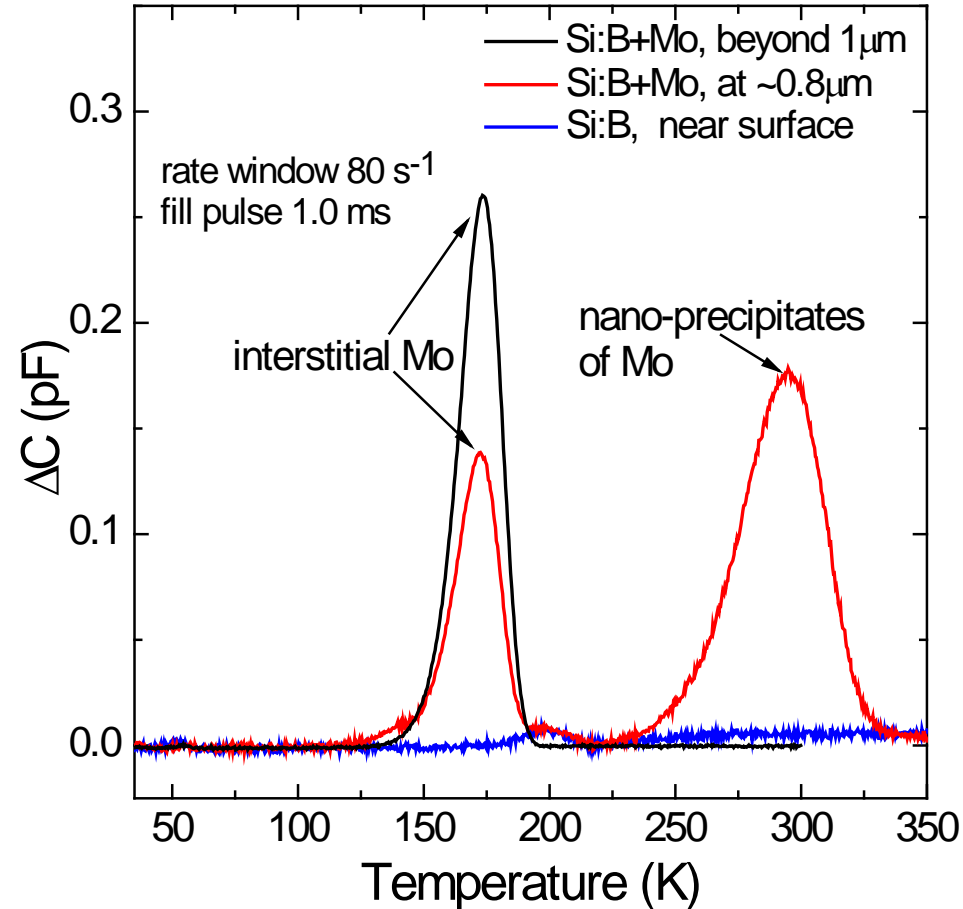
DLTS of Mo contaminated Epi Si

The interstitial Mo peak has electronic properties identical to those reported in the literature with (hole emission $\Delta E = 0.3\text{eV}$)

An energy level due to nano Mo is in the middle of the gap (hole $\Delta E = 0.47\text{eV}$)

The capture cross section of minority carriers (electrons) by nano-Mo defects is $>10^{-14}\text{ cm}^2$; two orders more than isolated interstitial Mo but with a smaller majority carrier cross section dependent on minority carrier population. So, the nano-Mo defects are very strong recombination centres showing no saturation

In this sample there is a band of Mo contamination deliberately introduced



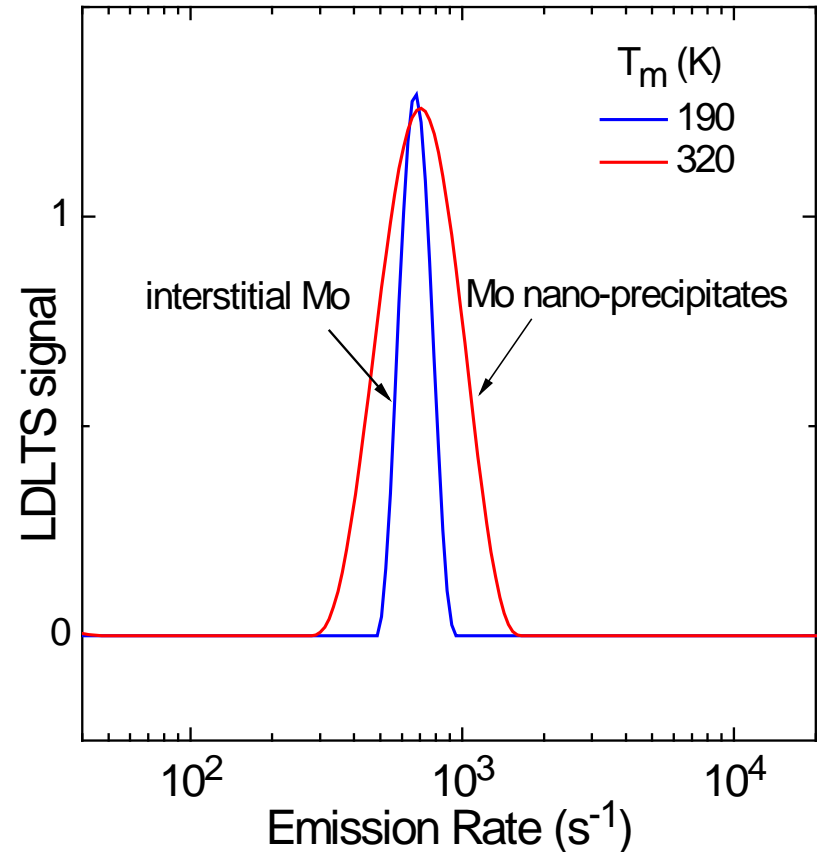
LDLTS of Epi

Laplace DLTS removes the instrumental broadening from DLTS so the linewidth has physical meaning

Comparing the hole emission from the Mo related nano-precipitates and single interstitial Mo atoms. **the nano-precipitate peak is significantly broader ... very different to a point defect.**

This could be due to an ensemble of sizes or inhomogeneous strain

For comparison different measurement temperatures are used to super-imposed the spectra. The thermal broadening is insignificant.



Recombination in Cast Silicon

Two major problems in applying our techniques to cast material:

- 1) Wide variation in material between manufactures and within an ingot.
- 2) Localised strain (seen in Raman spectroscopy), near precipitates and dislocation clusters, shifts and broadens DLTS signals making identification of defects difficult in many regions of the crystal.

Evidence from DLTS measurements that some regions have recombination behaviour typical of the rather unusual behaviour of nano-precipitates.

Kerfless Silicon

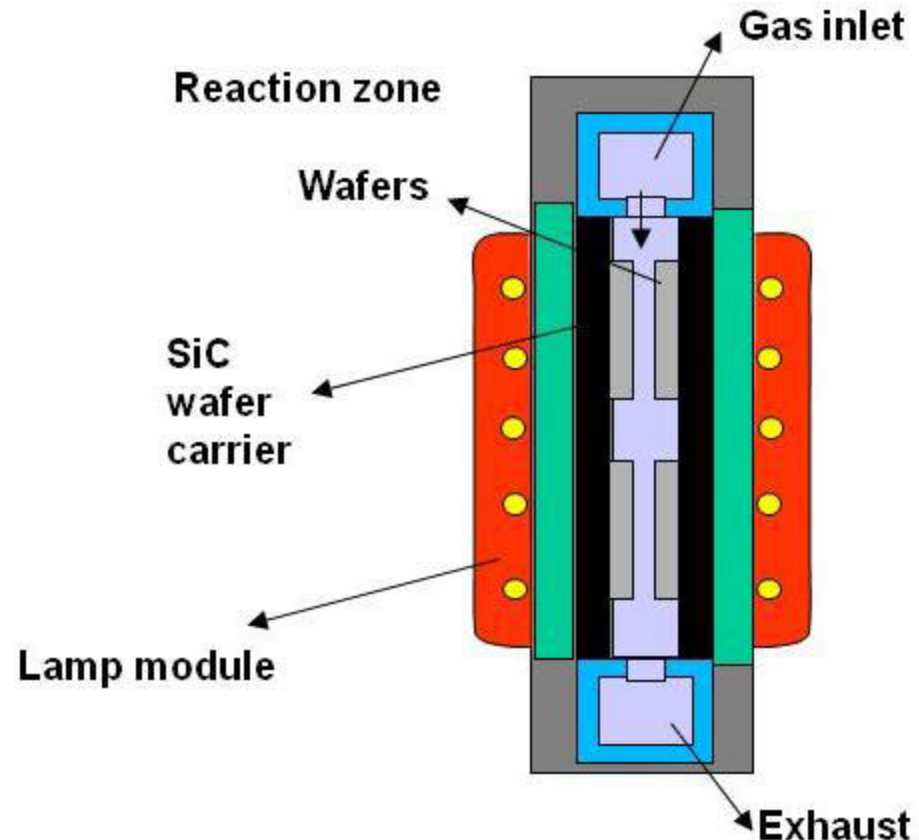
Kerfless silicon is grown as slices and needs no cutting or polishing. Historically all kerfless slices exhibit poor lifetime

Crystal Solar has developed the Canon ELTRAN process to grow single crystal slices on a porous silicon bi-layer. The epi layer (~80 μ m thick) is released from the square substrate which is reused

Tony Buonassisi group at MIT have worked with Crystal Solar to try to increase the lifetime of the layers
Powell et al APL 103, 263902 (2013)

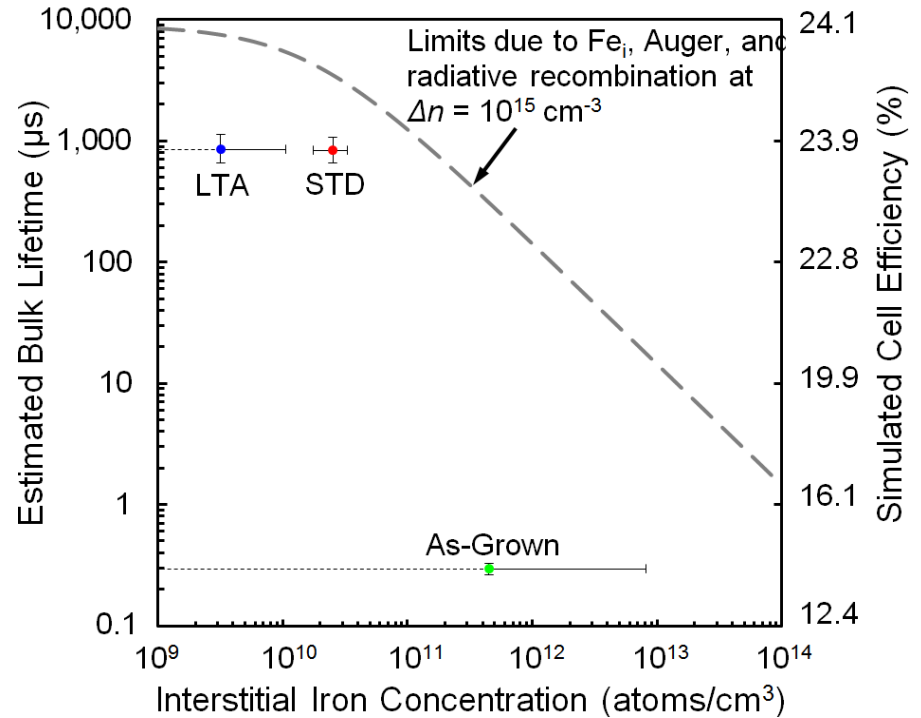
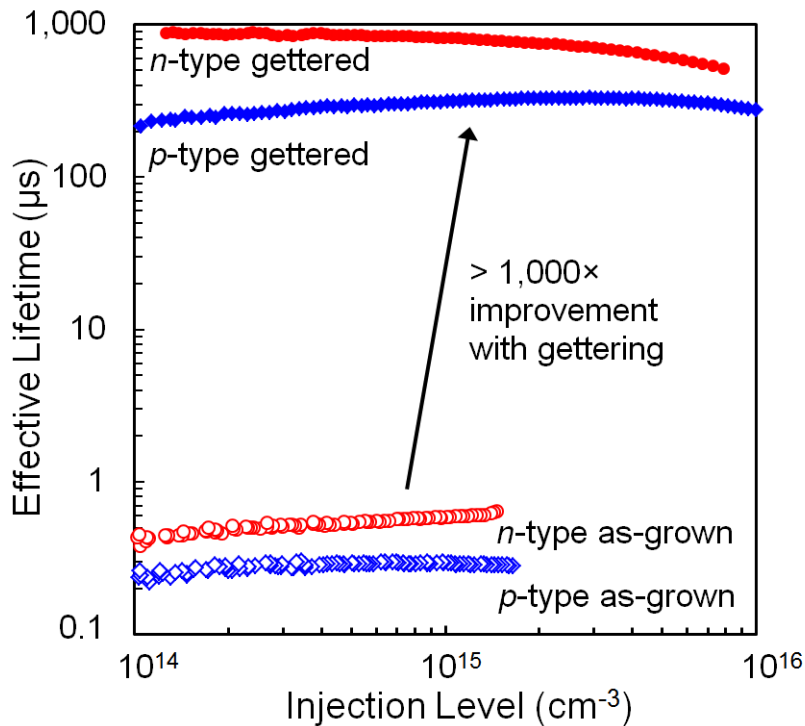
It was found that gettering improved the lifetime dramatically. We joined the collaboration and discovered a very unusual lifetime killer.

Crystal Solar epi growth furnace using trichlorosilane to grow at >4 μ m/min. Each furnace can produce 500 slices/hour



Kerfless silicon ... gettering

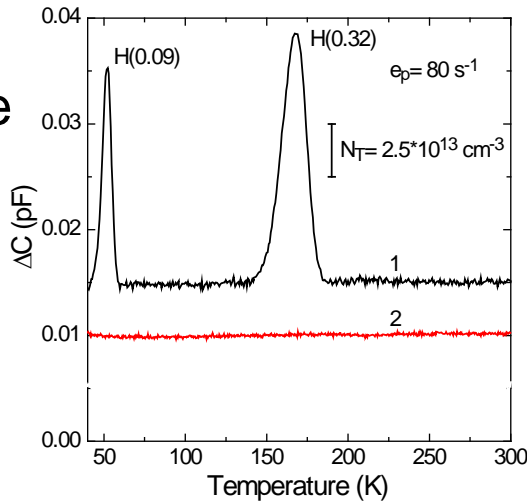
MIT's gettering process (POCl_3 845°C for 25min) had a dramatic effect on the lifetime which could not be attributed to Fe



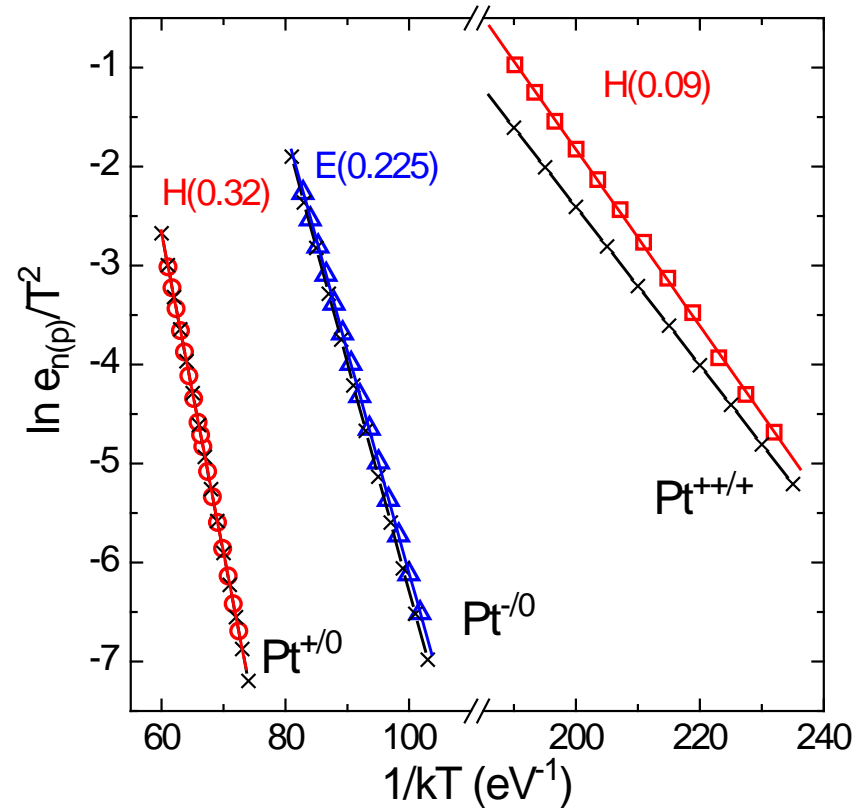
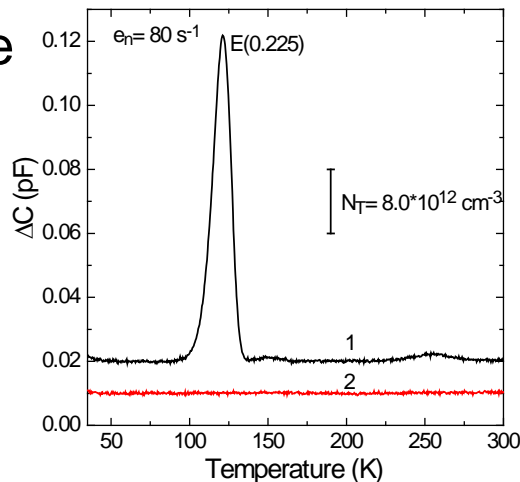
Kerfless silicon ... DLTS

DLTS shows that the recombination centre is Pt which can be seen in the epi in three charge states and also as PtH when hydrogenated.

p-type



n-type



Arrhenius plots of emission from deep states seen in epi with literature values for Pt (black crosses)

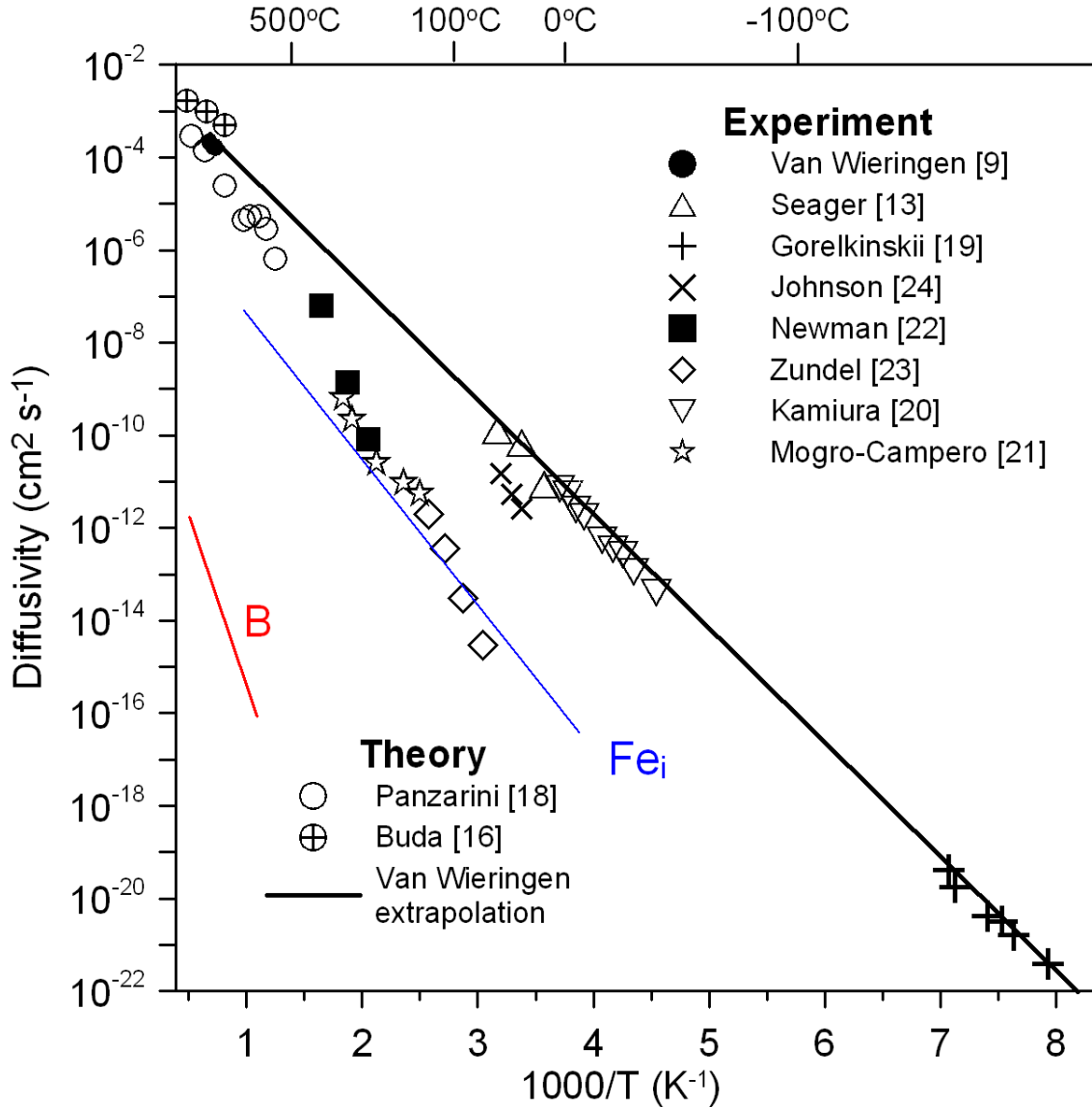
Hydrogen passivation

Hydrogen is a very reactive species which diffuses rapidly in silicon and so is expected to be a very effective passivator. It is central to surface and interface passivation in solar and MOS technologies but there is no consensus on its role as a passivator of the 3d transition metals in the bulk.

Hydrogen diffuses as an isolated ion: H^+ in p-type and intrinsic Si and H^- in n-type ... it has negative U properties so H^0 is metastable. H^+ bonds to ionised acceptors and H^- to donors so hydrogen compensates all shallow dopants very effectively. These complexes have weak binding BH 1.28eV and PH 1.32eV so dissociate $\sim 150^\circ\text{C}$ and act as a source of hydrogen for other reactions.

The passivation of the substitutional 5d TMs is now quite well understood but reactions with the important 3d metals which are thought to be mostly interstitial present conflicting results in both experimental and theoretical studies. We are trying to find out why

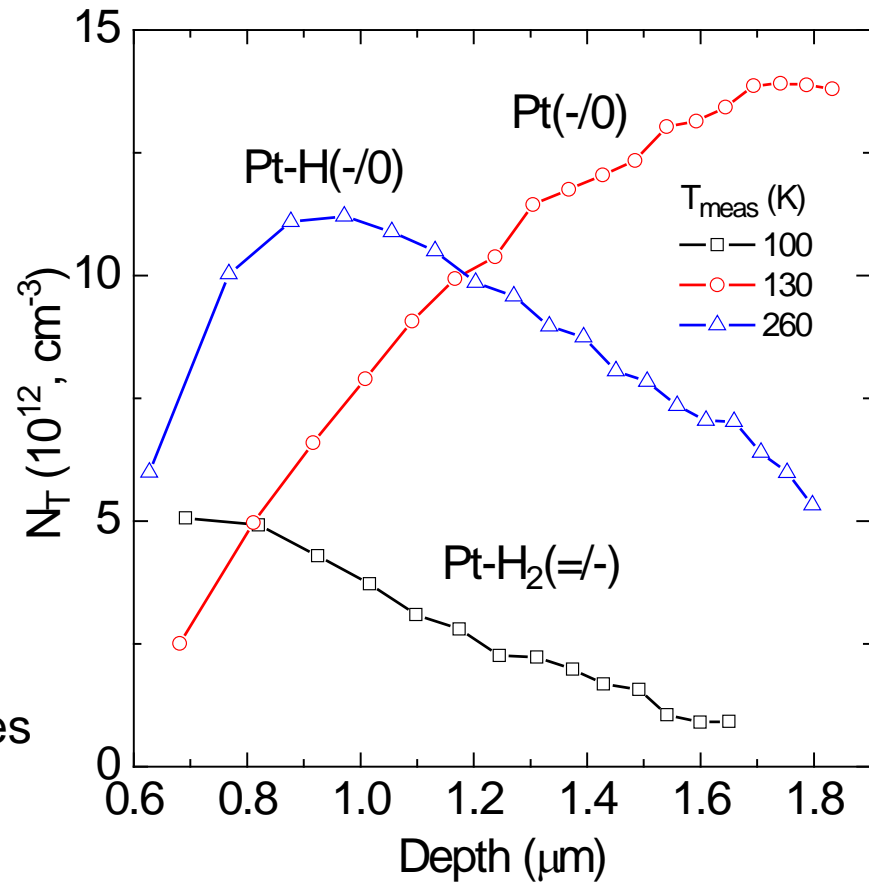
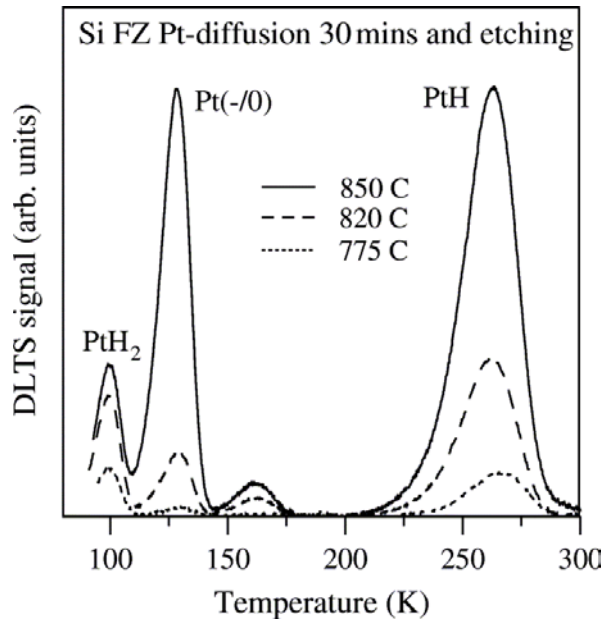
Diffusion of hydrogen in silicon



Very fast diffuser but large discrepancies in experimental values due to trapping at various defects.

Diagram from Peaker and Markevich "Hydrogen related defects in Si, Ge and SiGe" Ch 2 in "Defects in Microelectronic Materials and Devices" eds Fleetwood et al CRC Taylor and Francis 2009

Example: Spatial profiles n-Si:Pt DLTS Schottky diodes on HF-etched surface



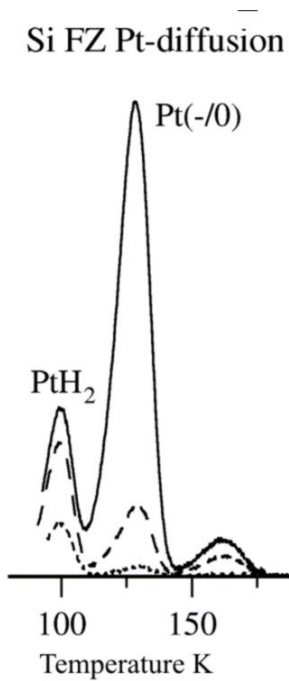
Pt diffused then wet etched

Pt is a 5d transition metal and occupies a substitutional site in silicon. Stable hydrogen complexes have been observed with passivation being achieved with 4 hydrogen atoms

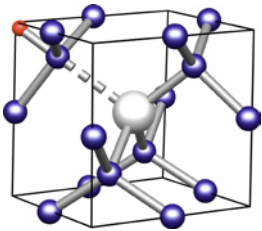


very similar behaviour is observed for Au. Complexes dissociate >180°C

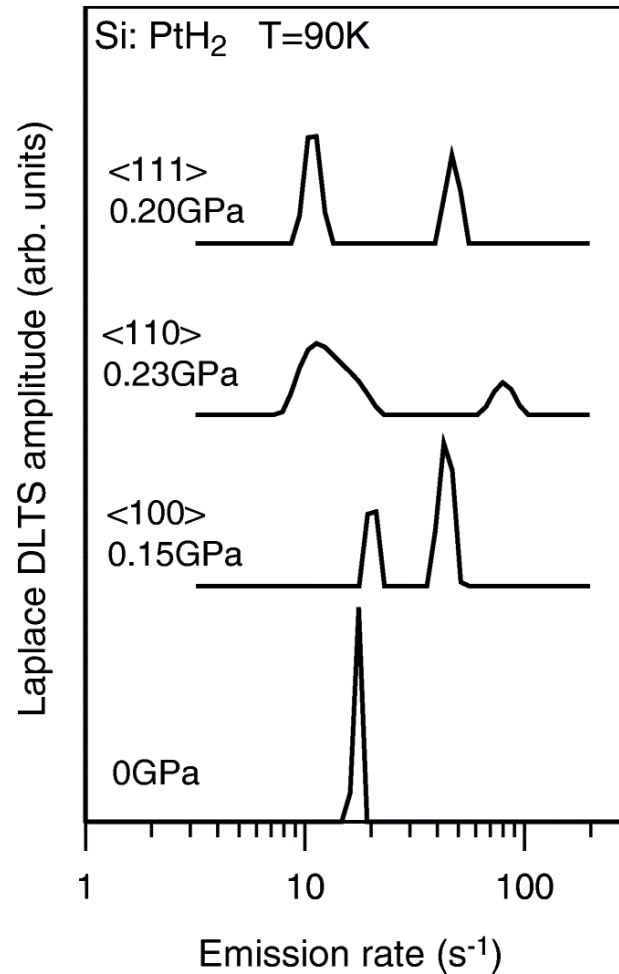
Example: structure of $\text{Si:PtH}_2^{-/-}$



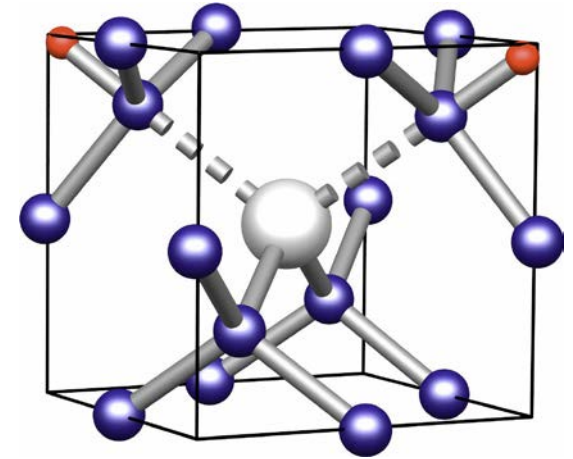
Pt diffused then wet etched



Pt → PtH →



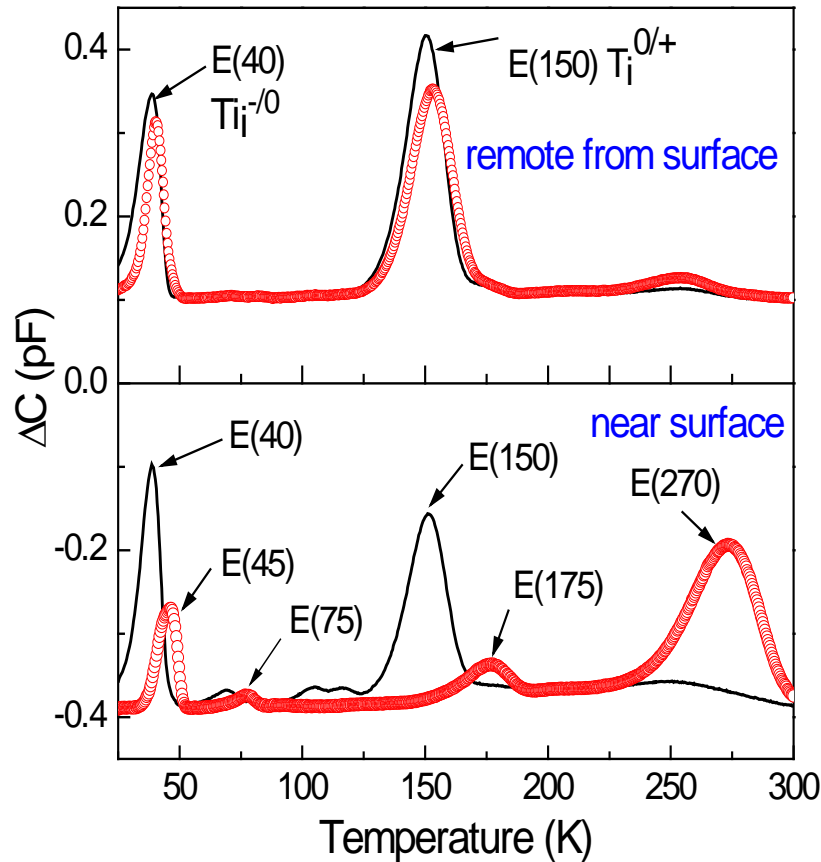
PtH₂



Splitting shows orthorhombic C_{2v} symmetry. Pt atom shown grey with hydrogen (red) in anti-bonding positions. We have used LDLTS to analyse both paramagnetic and diamagnetic states (not possible with EPR) and find a re-orientation energy of 1eV ie no re-orientation at RT and below.

Kolkovsky et al PRB 73, 195209 (2006)

Example: Si:TiH



Mg 12	3d transition metals										Al 13
Ca 20	Sc 21	Ti 22	V 23	Cr 24	Mn 25	Fe 26	Co 27	Ni 28	Cu 29	Zn 30	Ga 31
Sr 38	Y 39	Zr 40	Nb 41	Mo 42	Tc 43	Ru 44	Rh 45	Pd 46	Ag 47	Cd 48	In 49

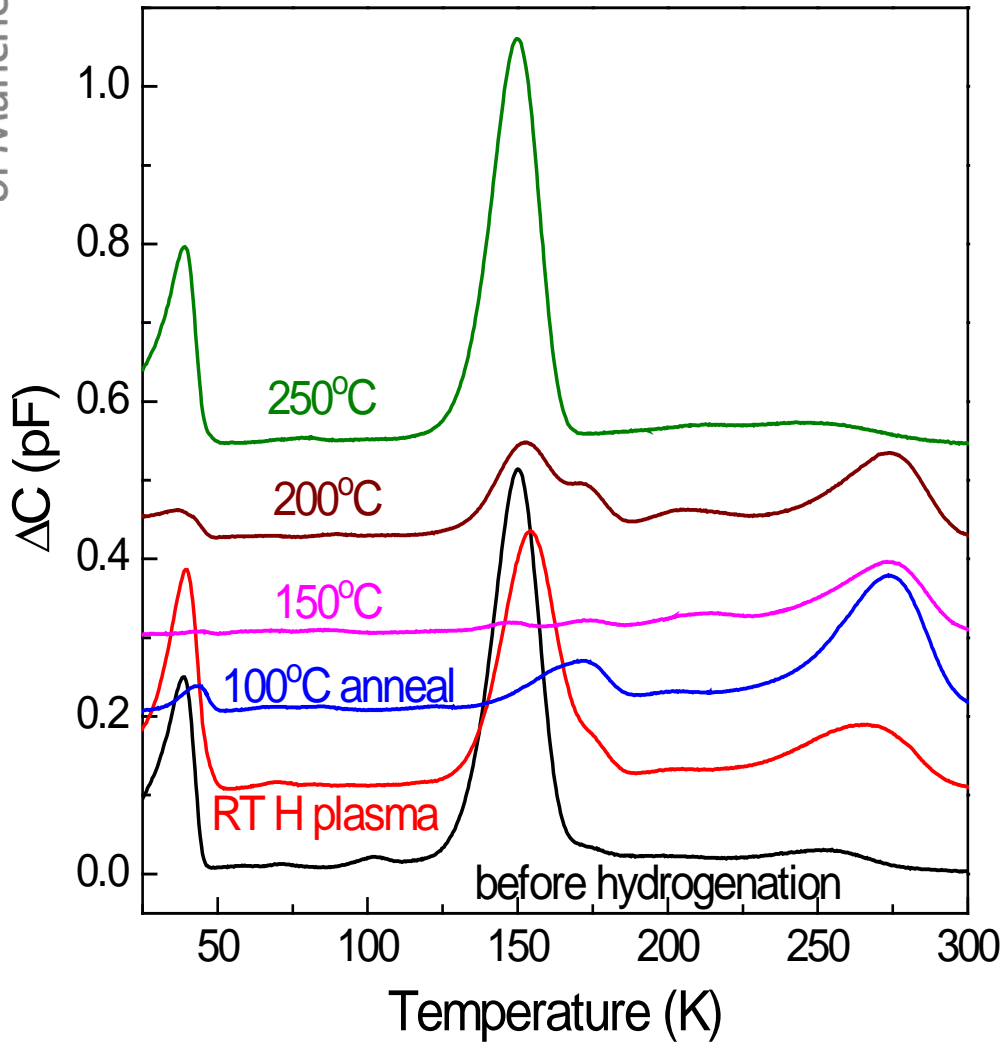
Ti slow diffuser so passivation is very important It is predominantly interstitial but with a fraction on substitutional sites. It forms electrically active complexes with H Theory suggests two different TH defects but with TiH_2 and TiH_3 being energetically unfavourable. TiH_4 is predicted to exist and to be electrically inactive

Leonard et al APL 103, 132103 (2013)

Markevich et al APL 104, 152105 (2014)

DLTS of implanted Ti annealed 650°C 30min (black) and + remote H plasma 60min (red)

Example: Si:TiH



DLTS of implanted Ti annealed 650°C 30min (black) and + remote H plasma 60min (red) at RT then 30min anneals

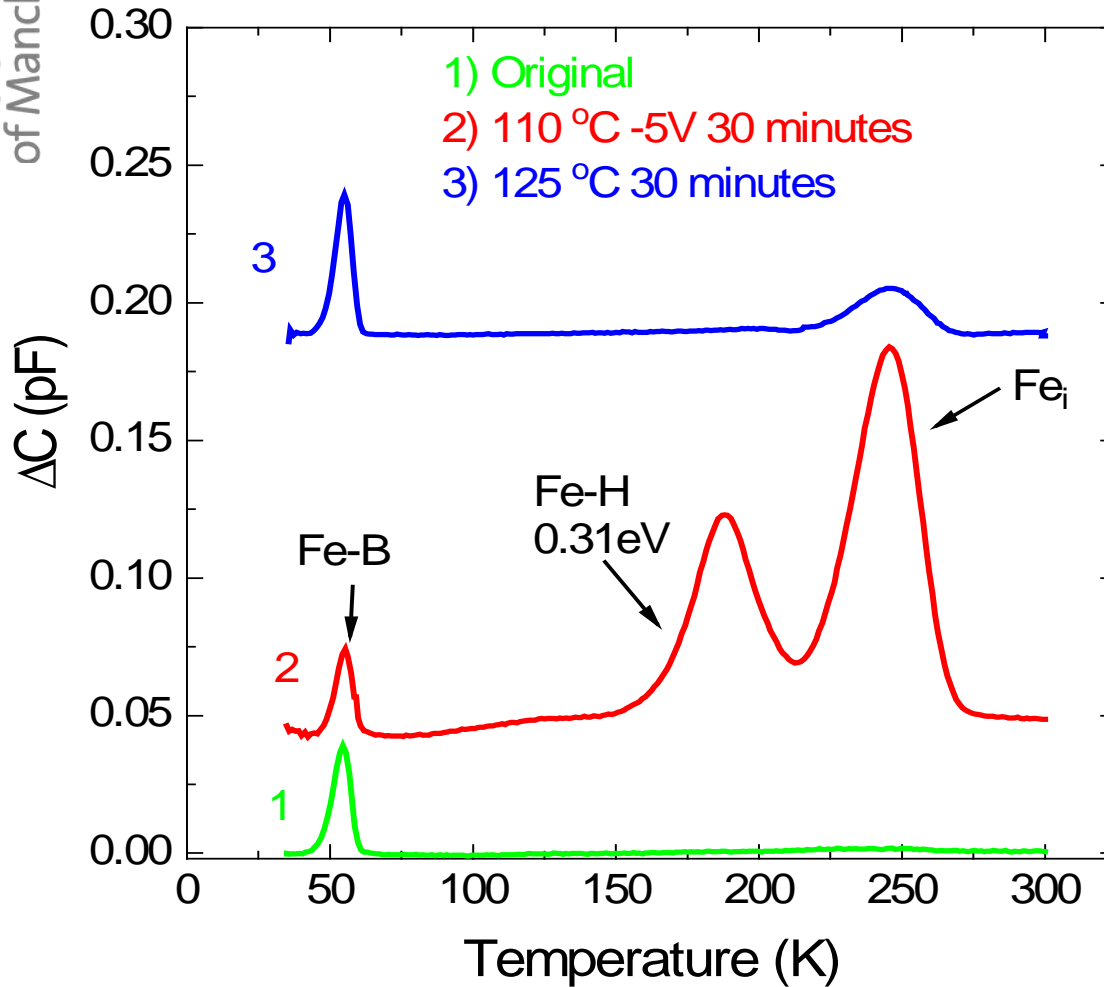
TiH forms during annealing due to migration of hydrogen. At 150°C almost total passivation is achieved but at 200°C the complex dissociates until at 250°C all the hydrogen bonded to Ti is lost and the Ti recombination is reactivated.

Generally assumed Fe is interstitial despite many interpretations of EPR and Mossbauer experiments as well as theory suggesting Fe_s can exist. An experiment from ISOLDE using emission channelling confirms Fe_s in implants and under some anneal conditions can be the dominant form of Fe. **Is Fe_s the reason some data on Fe appears inconsistent?**

Most theorists agree that Fe_i cannot be passivated with H indeed Fe_iH seems to be a more powerful recombination centre than Fe_i . **Theory** suggests that all Fe_iH complexes are electrically active with weak binding $\sim 0.8eV$. But there is strong **experimental** evidence for the passivation of Fe with hydrogen

We see one electrically active FeH complex and that dissociates at $125^{\circ}C$. We see no evidence of loss of electrical activity of Fe at following low temperature hydrogenation cycles

Formation and dissociation of Fe_iH in p-type Si



Cz sample with Fe diffusion and then H incorporation from SiN_3 followed by anneals. The reaction between Fe_i and H was effected in the depletion region of a Schottky diode

We would like to thank the UK Engineering and Science Research Council for funding this work. The support of the National Science Foundation (NSF) and the members of the Silicon Solar Consortium (SiSoC) for valuable discussions and the provision of samples are also gratefully acknowledged.

Thank you!